

## **PS-wave azimuthal anisotropy in a North American carbonate basin**

*Bruce Mattocks, Jianchao Li, Steve Roche, and Shuki Ronen*

*Veritas DGC Inc.*

### **Summary**

In an onshore example from a US carbonate basin, an embedded multicomponent test exhibits good PS-wave signal quality at the depth of interest, and all the expected characteristics of converted waves in azimuthally anisotropic media. In particular, there are clear azimuthal polarity reversals on the transverse receiver component, separated by null amplitudes defining the symmetry planes of the natural coordinate system; azimuthal velocity variations on the radial component then distinguish the specific symmetry plane aligned with maximum horizontal stress. The cumulative anisotropy is in good agreement with regional horizontal stress from borehole breakouts.

## Introduction

While the orientation and distribution of fractures cannot be directly imaged by seismic surveys, characteristics related to fracturing can be inferred from the azimuthal variations of seismic attributes. The same physical phenomena that create azimuthal amplitude variation (AVOA) in P-waves will generate azimuthal velocity variation and shear-wave birefringence in PS-waves. Converted-wave birefringence also resolves the inherent 90-degree ambiguity in fracture orientations determined by P-wave AVOA analysis alone (Rüger, 1998).

Nonetheless, the viability of PS-wave acquisition in any specific geological environment or geographical location is often in doubt. An embedded multicomponent test, where conventional geophone groups are replaced or co-located with single three-component (3-C) MEMS (Micro-ElectroMechanical System) sensors, can be a cost-effective method of evaluating this technology.

In this onshore US example, the fundamental goals were to determine the essential practicality of acquiring converted-wave data in gas-bearing hydrothermal dolomites at a depth of approximately 2750 m, and to evaluate the capacity of the PS-wave data to determine the orientation of horizontal stress. To minimize the cost of this PS-wave evaluation, the acquisition was implemented as an embedded multicomponent test, where Sercel DSU3 three-component digital accelerometers are co-located with production single-component geophone arrays over a subset of the P-wave survey area. The resulting eight square kilometer PS-wave image is approximately centered on a recent well in which a dipole sonic and FMI log were acquired.

## Data Acquisition

In those areas where the feasibility of converted-wave acquisition is in question, a small, embedded multicomponent test can be an economical means of appraising current technology. This study incorporates more than 1200 source points, and the 544 multicomponent receivers occupy a stationary patch within the larger 3-D project area. The general topography of the 3-D survey area and the layout of sources and receivers are illustrated in Figure 1. Conventional 10 Hz geophones, deployed in linear arrays of six elements, were used for the primary P-wave recording, while 3-C digital MEMS sensors were used for the embedded test. The 3-C receiver line interval is 503 m, co-located with the conventional geophone array line; however, the 3-C station interval is 33.5 m, or one-half the conventional geophone group interval of 67 m. The multicomponent receivers are active for all shots as a stationary spread

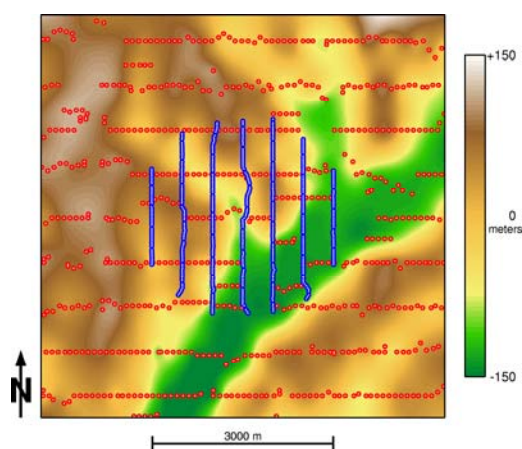


Figure 1: Surface topography, displayed as relative elevation, with source lines oriented east-west (red circles) and receiver lines north-south (blue circles).

	Conventional single component P-wave survey	Embedded multicomponent test spread
Survey extent	23 sq km	8 sq km
Receiver type	geophone	3C digital MEMS sensor
Array	6 elements over 20 m	single sensor
Receiver station interval	67 m	33.5 m
Receiver line interval	503 m	503 m
Active lines	14	7
Active stations	1848	544
Source type	dynamite	dynamite
Source interval	100 m	100 m
Source line interval	738 m	738 m

Table 1: Acquisition parameters for the conventional P-wave 3-D survey and embedded multicomponent test. The active geophone recording spread moved or “rolled” across the survey area, centered on the dynamite source point. The 3-C test spread remained stationary.

while the conventional geophone recording spread rolls across the survey extents. These parameters are summarized in Table 1.

### Converted-wave azimuthal anisotropy

The basic anisotropic characteristics of the converted-wave data are identified early in the processing sequence. The PS-wave data are initially processed in a conventional, isotropic manner. After correction for tilt and orientation, the receivers are rotated from the global acquisition coordinate system to a radial-tangential coordinate system, local to each source-receiver pair. Source and receiver statics are surface-consistent, while deconvolution operators are designed independently on each trace. Asymptotic Conversion Point (ACP) binning is used to preserve surface-consistent relationships for iterative velocity analysis with residual statics. Following normal moveout correction, a large superbin (600 m radius) is selected from the ACP-binned data for the initial evaluation of azimuthal anisotropy. The binned data are sorted and sub-stacked over ten-degree azimuth sectors.

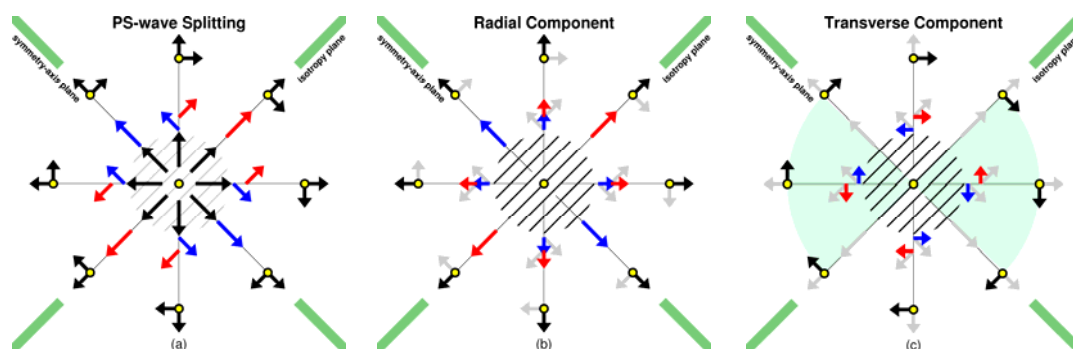


Figure 2: Schematic representation of PS-wave splitting, with the effective source at the center, receivers distributed azimuthally, and open fractures oriented N45°E. (a) The radially-oriented P-SV wave (black) splits into a fast P-S1 wave (red) parallel to the fractures and a slow P-S2 wave (blue) orthogonal to the fractures; (b) their projection on the radial receiver component displays a consistent polarity for all azimuths, but with variable arrival times; (c) on the transverse receiver component there is no projection in the isotropy plane or symmetry-axis plane (parallel and perpendicular to the fractures, respectively) and a polarity reversal (shaded) occurs across those planes.

Li (1998) describes the general characteristics of PS-wave data in azimuthally anisotropic media. For converted-wave acquisition, the effective source is a radially-oriented P-SV wave (Figure 2a) that splits, possibly instantaneously, into fast and slow shear-waves polarized in the fixed natural coordinate system. Since the data are initially processed in a local, radial-tangential, coordinate system, it is the projection of these split shear-waves on the individual radial and transverse receiver components that is of interest.

When the incident P-wave is aligned with the symmetry planes of the natural coordinate system, a radial P-SV wave reflection is generated (Figure 2b) but no shear-wave birefringence is observed and no reflection is visible on the transverse receiver component (Figure 2c). At intermediate azimuths this radial P-SV wave is split into a fast shear-wave aligned with open fractures, and an orthogonal slow shear-wave, both of which have projections on the radial and transverse receiver components

The projection on the radial component maintains a consistent polarity for all azimuths (Figure 2b); however, the travel-times vary azimuthally with the fastest arrival parallel to the open fractures. In contrast, the polarity of the projection on the transverse component (Figure 2c) reverses across the symmetry planes. As a result, the orientation of the symmetry planes can be determined by identifying the nulls separating azimuthal polarity reversals on the

transverse component. The isotropy plane (fast shear-wave) can then be distinguished from the symmetry-axis plane (slow shear-wave) by the travel-times on the radial component.

### Data Example

The azimuth stacks of this dataset demonstrate all the expected characteristics of azimuthally anisotropic PS-waves. Figure 3 shows  $10^\circ$  azimuth-sectored sub-stacks generated from the single ACP superbin, following the initial surface-consistent statics and velocity analysis. The radial component displays azimuthal variation in the arrival times of the various reflections, with the fastest arrivals occurring approximately east-west. The transverse component — which would be free of reflections in isotropic media — shows clear polarity reversals separated by amplitude nulls that define the orientation of the symmetry planes as  $N80^\circ E$  and  $N170^\circ E$ . The isotropy plane is then identified by the fast arrival on the radial component at  $N80^\circ E$ .

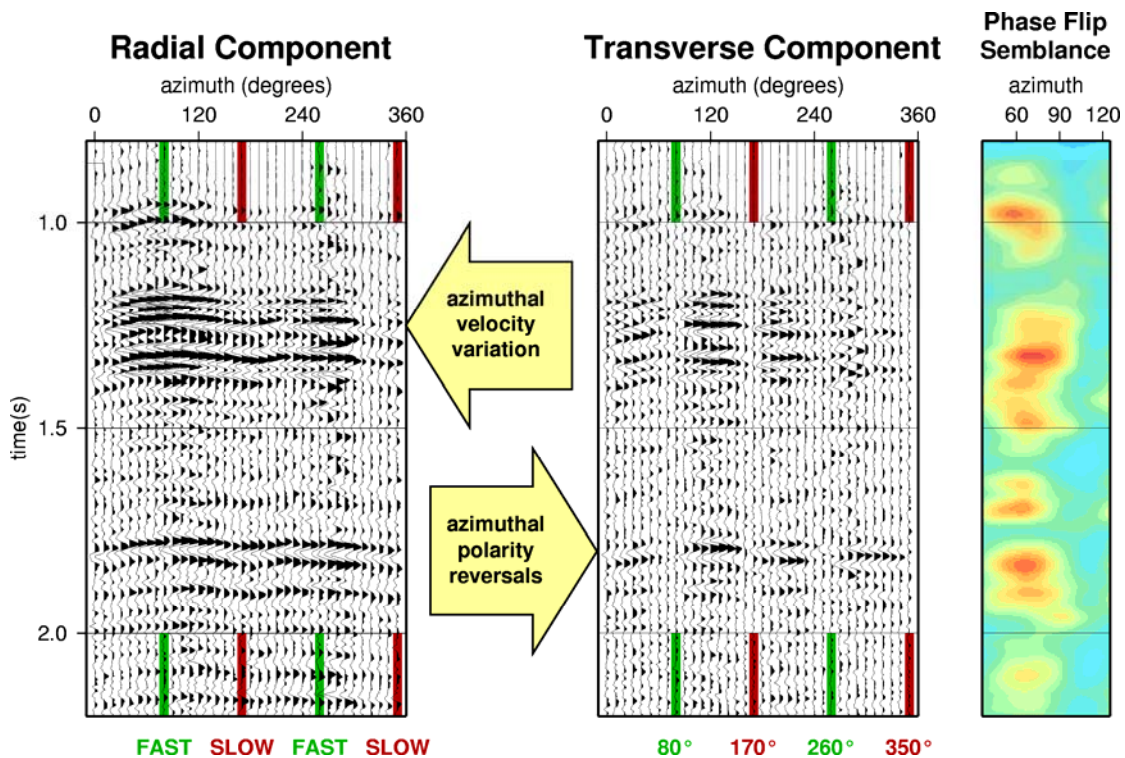


Figure 3: Radial and transverse azimuth stacks from a single ACP superbin, with the orientation of the symmetry planes shown in green (isotropy plane) and red (symmetry-axis plane). The data are sorted by azimuth, and each trace represents a sub-stack over a  $10^\circ$  azimuth sector. At right is the corresponding phase-flip semblance display.

Based on the polarity flips in the transverse component, the orientation of the symmetry planes can also be determined by calculating semblances for a range of possible directions (Bale et al, 2000). Figure 3 includes the corresponding “phase-flip semblance” plot, which permits the fast shear direction to be determined graphically. This plot also suggests the presence of temporal variations in the orientation of the symmetry planes, which in turn implies that the orientation of maximum horizontal stress might be changing with depth. However, such variations cannot be evaluated directly from this specific figure, which depicts only the cumulative anisotropy from surface. Layer-stripping is required to remove the effects of shallow anisotropy and reveal the interval anisotropy at depth (Winterstein and Meadows, 1991).

Using a smaller (240 m diameter) bin, the analysis is extended spatially and the anisotropy evaluated after rotating the data into the natural coordinate system; the results are summarized in Figure 4. Again, these results represent the cumulative anisotropy above the reservoir.

Nonetheless, the average orientation is consistent with the regional orientation of maximum horizontal stress from borehole breakouts (Figure 5).

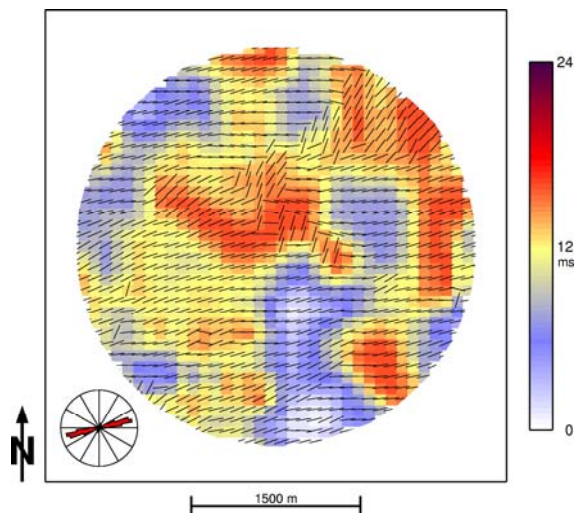


Figure 4: *Converted-wave birefringence above the reservoir, showing the fast shear polarization (vectors) and cumulative slow shear delay-time (color). Cumulative anisotropy is less than 3%.*

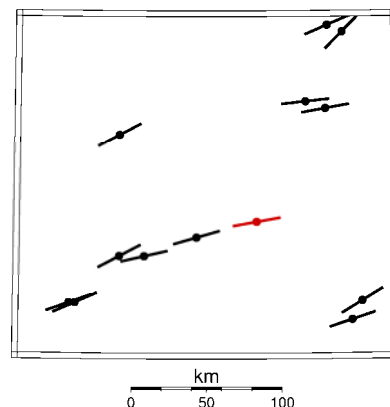


Figure 5: *Regional stress: the average fast shear-wave polarization from the PS-wave survey is shown in red and borehole breakout orientations from the World Stress map project (Reinecker et al, 2004) are in black. The median PS-wave polarization is N77°E, and the median breakout orientation is N69°E. Note the scale.*

## Conclusions

An embedded multicomponent seismic test provides an effective means of evaluating current converted-wave technology in an untested area. In this example, the limited PS-wave dataset exhibits adequate signal-to-noise ratio at the depth of interest, clear shear-wave birefringence, and unambiguous symmetry-plane orientations to complement AVOA results.

## Acknowledgements

We thank Nick Henderson and Bob Winarsky for processing these data. John Gibson, Richard Bale and Dragana Todorovic-Marinic provided valuable technical advice. We also thank the anonymous client for permission to present these results.

## References

- Bale, R., Dumitru, G., and Probert, T. [2000] Analysis and stacking of 3-D converted wave data in the presence of azimuthal anisotropy. 70th Ann. Internat. Mtg., Soc. Expl. Geophys., Expanded Abstracts, 1189–1192.
- Li, X.-Y. [1998] Fracture detection using P–P and P–S waves in multicomponent seafloor data. 68th Ann. Internat. Mtg., Soc. Expl. Geophys., Expanded Abstracts, 2056–2059.
- Reinecker, J., Heidbach, O., Tingay, M., Connolly, P., and Müller, B. [2004] The 2004 release of the World Stress Map (available online at [www.world-stress-map.org](http://www.world-stress-map.org)).
- Rüger, A. [1998] Variation of P-wave reflectivity with offset and azimuth in anisotropic media. *Geophysics*, 63, 935–947.
- Winterstein, D. F., and Meadows, M. A. [1991] Changes in shear-wave polarization azimuth with depth in Cymric and Railroad Gap oil fields. *Geophysics*, 56, 1349–1364.